

# Histological and ultrastructural changes of the colon in dextran sodium sulfate-induced mouse colitis

XIAOJUAN XU<sup>1,2</sup>, SISI LIN<sup>1</sup>, YANHUA YANG<sup>3</sup>, XIAOHUI GONG<sup>2</sup>,  
JIANHUA TONG<sup>4</sup>, KUN LI<sup>1</sup> and YONGYU LI<sup>1</sup>

<sup>1</sup>Department of Pathology and Pathophysiology, Tongji University School of Medicine, Shanghai 200092;

<sup>2</sup>Key Laboratory of Arrhythmias of the Ministry of Education of China, Shanghai East Hospital,

Shanghai 200120; <sup>3</sup>Department of Pathology, Qingdao Municipal Hospital, Qingdao,

Shandong 266011; <sup>4</sup>Shanghai East Hospital, Institute for Biomedical Engineering and Nano Science, Tongji University School of Medicine, Shanghai 200092, P.R. China

Received August 17, 2019; Accepted April 24, 2020

DOI: 10.3892/etm.2020.8946

**Abstract.** Ulcerative colitis (UC) is a complex disease that results from a dysregulated immune response in the gastrointestinal tract. A mouse model orally administered with dextran sodium sulfate (DSS) is the most widely used experimental animal model of UC. However, the ultrastructure of the colon in mouse colitis is poorly understood. In the present study, colonic specimens from DSS-induced UC mice underwent hematoxylin and eosin staining, Masson's trichrome staining and Verhoeff's elastic staining. In addition, the ultrastructure of samples was examined by transmission electron microscopy. UC was successfully induced by 7 consecutive days of DSS oral administration. The goblet cell architecture of the UC tissue was damaged in the mucosa. Additionally, a significant number of inflammatory cells infiltrated into the stroma and the structure of the intestinal gland was destroyed. The tissue in the submucosa showed significant edema. Hyperplasia was also identified in the submucosa, promoting a disorganized microstructure within the colon wall. Numerous collagen fibers in the muscular layer were disrupted, and the fiber bundles were thinner compared with those in the normal control group. Furthermore, in the DSS-induced UC group, the smooth muscle cell showed edema, the cell membrane structure was unclear and the shape of the nucleus was irregular. In conclusion, the present study revealed important histological and ultrastructural changes in the colon of DSS-induced UC mice. These features may contribute to improved understanding of the pathogenesis and mechanism of UC.

## Introduction

Ulcerative colitis (UC) is one of the typical complex inflammatory bowel diseases (1). Major clinical manifestations of UC include abdominal pain, diarrhea, vomiting and weight loss, with the hallmark clinical symptom of UC being bloody diarrhea (2). UC is influenced by genetic, environmental, immunoregulatory and microbial factors (3). Unlike Crohn's disease (CD), UC is a mucosal disease that always affects the rectum and could spread up to the cecum with a continuous retrograde distribution (4). UC is characterized by chronic relapsing intestinal inflammation that eventually leads to extensive tissue fibrosis and a stiff colon that is unable to perform peristalsis or resorb fluids (5,6). In early fibrotic UC cases, fibrosis affects the muscularis mucosae and submucosa, while the muscularis propria is not affected. In advanced fibrotic UC cases, fibrosis extends to affect the muscle layers and the myenteric plexus (7).

The establishment of an animal model is required for efficient study of etiology, diagnosis, treatment and novel drug discovery in UC. Previous studies have induced UC in animals by a variety of methods including acetic acid, carrageenan, dextran sodium sulfate (DSS) and dinitrochlorobenzene (8,9). In particular, the DSS-induced murine model has been widely used in UC-related experimental investigations (10,11). In these previous studies, the pathological alterations were characterized as epithelial erosion and ulceration, submucosal edema and infiltration of neutrophils into the lamina propria and submucosa, which is similar to what occurs in human UC (12). While the histological and ultrastructural features in the DSS-induced UC model remain to be elucidated, improving the understanding of pathological characteristics of the model is likely to offer further insight into UC research (13). Histological and ultrastructural investigations were performed in a DSS-induced colitis murine model in the present study. Changes in the microstructure of the colon tissue in response to early stages of experimental colitis were also assessed.

## Materials and methods

**Mice.** A total of 30 specific pathogen-free female C57BL/10J wild type mice (age, 10-12 weeks; weight, 25-35 g) were

---

*Correspondence to:* Professor Yongyu Li, Department of Pathology and Pathophysiology, Tongji University School of Medicine, 1239 Siping Road, Shanghai 200092, P.R. China  
E-mail: liyongyu@tongji.edu.cn

**Key words:** dextran sodium sulfate-induced ulcerative colitis, colon, histology, ultrastructure

obtained from the Model Animal Research Center of Nanjing University. The mice were kept at the animal housing facilities (24±1°C; 12-h light/dark cycle; 55% humidity and ad libitum access to food and water) at Tongji University. All experimental procedures were performed according to international guidelines for the care and use of laboratory animals (14) and approved by the Animal Ethics Committee of Tongji University School of Medicine, Shanghai, China (approval no. TJLAC-014-015).

**Experimental colitis.** The mice were randomly divided into two groups: One healthy control group and one experimental UC group (n=15 mice in each group). DSS (36-50 kDa; cat. no. 160110; MP Biomedicals) was added to tap water at a concentration of 4%. Mice in the experimental UC group were exposed to DSS for 7 days (15). Healthy control animals drank tap water alone. The fresh stools of each mouse were collected each day for a total of 7 days. Stool scores varied from 0 (normal) to 3 (diarrhea) points based on stool properties such as shape, moisture, and viscosity (15).

**Colitis score.** Colonic damage was assessed according to the macroscopic score (MS). According to Li *et al* (15) and Kimball *et al* (16), the MS encompassed: i) Weight loss score; ii) colon length shortening score; and iii) the occult blood score. Each scoring system had four points in total. Thus, the MS was the sum of the three scores (0 points, most healthy; 12 points, least healthy).

**Specimen preparation.** Mice were sacrificed by cervical dislocation on the seventh day of colitis induction. The intestines were excised and carefully rinsed with saline. A 30-mm section of colon, which was considered to begin at a point 10 mm away from the caecum, was cut out and weighed. The colon was then dissected into two portions, with 10 mm (sample 1) allotted for histological analysis and 5 mm (sample 2) allotted for transmission electron microscopy (TEM). Sample 1 was fixed in 4% paraformaldehyde (Sigma-Aldrich; Merck KGaA) in 4°C for 24 h, while sample 2 was fixed in 2.5% paraformaldehyde and 2.5% glutaraldehyde in 0.1 M Na-Cacodylate buffer (pH 7.4; all from Sigma-Aldrich; Merck KGaA) in 4°C for 24 h. In total, 15 control and 15 UC tissue samples were collected to undergo histological analysis and TEM evaluation.

**Histology.** For histological investigation, sample 1 was washed with PBS and dissected into two portions. One of the portions was embedded in paraffin and sectioned at 5- $\mu$ m thickness on a Leica RM2126 microtome (Leica Biosystems). The sections were first deparaffinized and then stained with hematoxylin and eosin (H&E; Abcam) to assess the degree of inflammation according to the instructions from the manufacturer. Sections were stained with Masson's trichrome (Sigma-Aldrich; Merck KGaA) and Verhoeff's elastic staining (Abcam) to visualize the connective tissue according to the manufacturer's instruction. The other portion was embedded in optimal cutting temperature compound (Leica Biosystems) and sectioned at 10- $\mu$ m thickness on a Leica CM1860 microtome (Leica Biosystems). The sections were first washed with PBS and permeabilized in 0.025% Triton X-100 and 1% BSA in TBS buffer for 20 min at room temperature. Then the sections

were incubated overnight at 4°C with anti- $\alpha$  smooth muscle actin antibody (1:100; Abcam; cat. no. ab5694) in TBS buffer with 1% BSA, followed by labeling with Alexa 488-conjugated goat anti-rabbit IgG H&L (1:300; Abcam; cat. no. ab150077) in TBS buffer with 1% BSA at room temperature for 1 h. The sections were washed with PBS before using the mounting medium with DAPI (Abcam; cat. no. ab104139) in the dark. Tissue pathophysiology was characterized by the presence of ulcerations, inflammatory cells (such as neutrophils, macrophages, lymphocytes and plasma cells), signs of edema, crypt loss, surface epithelial cell hyperplasia, goblet cell reduction and signs of epithelial regeneration. The histopathological score (HS) was used as a method for evaluating the degree of UC lesions. The HS evaluation included: i) Crypt architecture damage score (0-2 points); ii) edema in submucosa score (0-3 points); and iii) inflammatory cell infiltration score (0-3 points). HS was the sum of the three scores (0 points, most healthy; 8 points, least healthy), based on previously published reports by Li *et al* (15) and Engel *et al* (17).

**TEM.** For TEM experiments, sample 2 was first washed with PBS, then fixed in 1% osmic acid in room temperature for 2 h, dehydrated by acetone and embedded in Spurr Embedding medium in 60°C for 48 h (Sangerbio). Subsequently, 70-nm sections were cut, stained with uranyl acetate for 20 min and lead citrate for 5 min in room temperature, and examined using JEOL-1010 transmission electron microscope (original magnification, x20,000; JEOL, Ltd.).

**Statistical analysis.** Experimental data are presented as the mean  $\pm$  SD. Shapiro-Wilk and Kolmogorov-Smirnov tests were used to determine data normality. Comparisons of the quantitative values between the control and UC groups were performed using Student's t-test. Mann-Whitney U test was used to analyze the ordinal data. P<0.05 was considered to indicate a statistically significant difference. Statistical analyses were performed using SPSS 21.0 statistical software (IBM Corp.).

## Results

**Mouse UC model.** During DSS feeding days, clinical symptoms of UC mice, such as loss of body weight, loose feces/watery diarrhea and fecal blood were noted. Macroscopically, the body weight loss of mice with UC was observed from day 2, and on day 7, the body weight loss score of UC mice was significantly higher compared with control mice (Fig. 1A). On day 3, several mice in the UC group began to experience diarrhea, followed by hematochezia. All UC mice had diarrhea and hematochezia on day 6. The length of the colon was measured at necropsy. As shown in Fig. 1B, the colon length shortening scores of UC mice were significantly higher compared with healthy mice. The occult blood scores of UC mice were significantly higher compared with healthy controls (Fig. 1C). The total MS of mice in the UC group was 9.3±0.3 points, while the control group total MS was 0 points (Fig. 1D). Thus, acute UC was successfully induced in C57BL/10J mice by oral administration of 4% DSS for 7 days.

**Histology.** H&E staining. H&E staining revealed structural changes of colon tissues of mice in control and UC groups

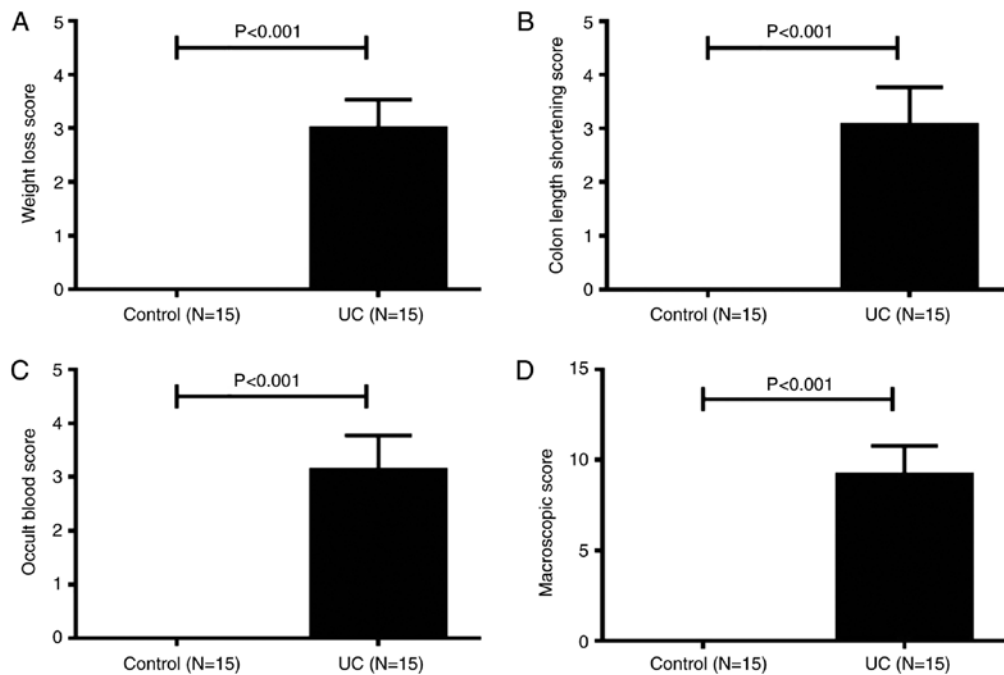


Figure 1. Macroscopic score of dextran sulfate sodium-induced colitis in C57BL/10J mice (A) Weight loss score. (B) Colon length shortening score. (C) Occult blood score. (D) Macroscopic score of mice colons. Data are presented as the mean  $\pm$  SD. UC, ulcerative colitis.

(Fig. 2A-D). A series of pathological changes occurred in the UC group (Fig. 2B and D) compared with the control group (Fig. 2A and C). In the mucosa, the goblet cell architecture of the colon tissue was damaged (as indicated by the stars in Fig. 2D). A number of inflammatory cells infiltrated into the stroma and the structure of the gland was destroyed (Fig. 2D). In the submucosa, the tissue presented with significant edema, which was mainly due to inflammatory cell infiltration (indicated by the arrows in Fig. 2D). In the muscularis propria, the smooth muscle cell structure was altered; the nuclei became rounder and the boundaries of the cells became indistinct. However, inflammatory cells were not found in this layer (Fig. 2D). The thickness of the muscularis propria of UC cells was significantly reduced compared with the control group (Fig. 2E), however, the whole thickness of the colon wall of UC mice significantly increased compared with the control group due to edema of the submucosa (Fig. 2F). There was no visible difference between the control and UC groups in the serosa. As shown in Fig. 2G, the HS for the UC group was  $6.2 \pm 0.2$  points, while the HS of the control group was 0 points. This result indicated that the lesion of colon in DSS-induced UC mice was significant.

**Masson's trichrome staining and Verhoeff's elastic staining.** Masson's trichrome staining and Verhoeff's elastic staining showed changes in the microscopic structure of the mouse colon wall. Masson's staining dyed the collagen fibers blue, the muscle cells red and the nuclei dark blue. The elastic staining dyed the elastic fibers black, the collagen fibers red, the muscle cells yellow and the nuclei blue to black.

Compared with the control group (Fig. 3A), a number of pathological changes occurred in the microstructure of the UC group (Fig. 3B) as revealed by Masson's trichrome staining. In the submucosa, the collagen fibers were scarce

in the UC group but tightly packed into bundles in the control group. Collagen fibers in the UC submucosa evidently presented with hyperplasia and the fiber alignment was more disordered compared with control. In the muscularis propria, collagen fibers in the control group surrounded the smooth muscle cells regularly. However, numerous collagen fibers in the UC muscular layer were disrupted and fiber bundles became thinner compared with the control group (Fig. 3A and B).

According to the results of elastic staining, the most notable difference between the control group (Fig. 3C) and the UC group (Fig. 3D) was the completeness and continuity of elastic fibers. In the muscularis propria, elastic fibers are produced by smooth muscle cells (18). In the submucosa, the collagen fibers of the UC group were proliferated and disordered (indicated by red arrows; Fig. 3D). In muscularis propria, the elastic fibers were continuous and arranged between the smooth muscle cells equally (indicated by black arrows; Fig. 3C) in the control group. However, in the UC group, the elastic fibers were rare, and the arrangement was irregular (Fig. 3D).

**Immunohistochemistry staining.** Staining with  $\alpha$  smooth muscle actin antibody specifically stains the smooth muscle cells. There are two muscle layers in the mouse colon wall: Muscularis mucosa and muscularis propria. The latter muscle cells are divided in two groups: Longitudinal muscle and circular muscle (19). In the control group (Fig. 3E), the smooth muscle cells in the muscularis mucosa and muscularis propria exhibited normal morphology. The cells were long and spindle-shaped, the size was uniform, the cell membrane was clear, the cell edge was distinct and the cell nucleus was spindle-shaped (Fig. 3E). By contrast, smooth muscle cells in the UC group were rounder and shorter and the membranes

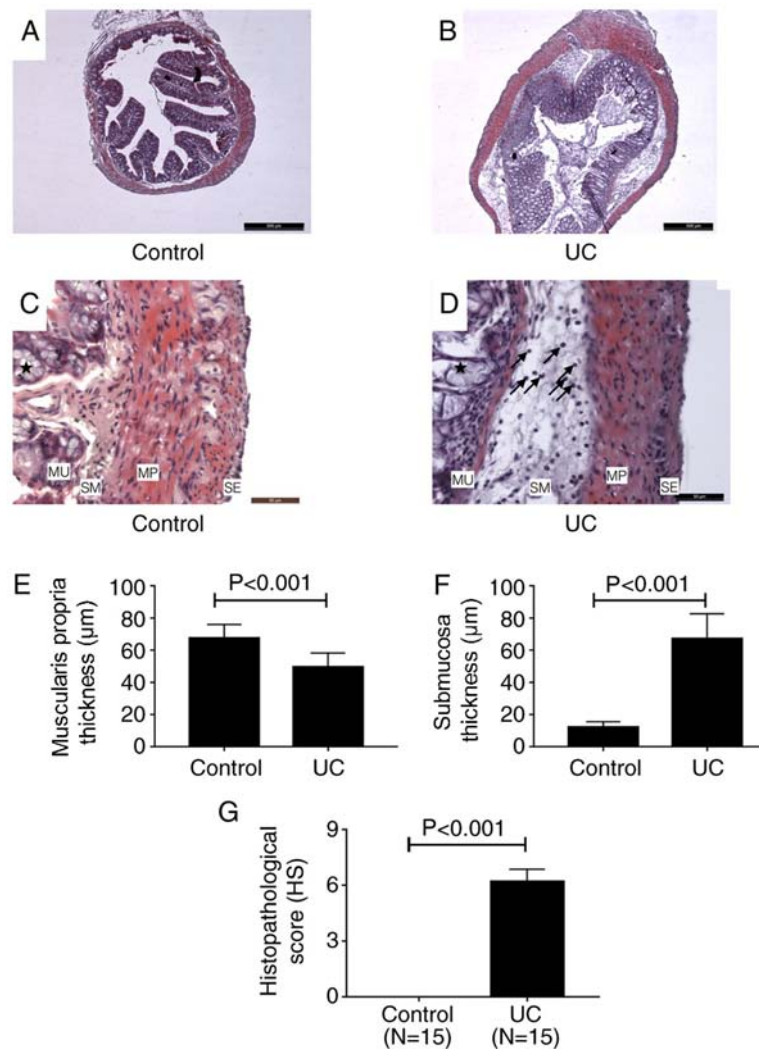


Figure 2. Hematoxylin and eosin staining of colon tissues. Images of (A) control and (B) UC tissues at x40 magnification. Scale bar, 500  $\mu\text{m}$ . Images of (C) control and (D) UC tissues at x400 magnification. Scale bar, 50  $\mu\text{m}$ . Goblet cells are indicated by stars. The black arrows indicate the inflammatory cells infiltrating into submucosa. Thickness of the (E) muscularis propria and (F) submucosa in control and UC mice. (G) Histopathological score of control and UC mice. UC, ulcerative colitis; MU, mucosa; SM, submucosa; MP, muscularis propria; SE, serosa.

were not as distinct as those in the control group. Additionally, the muscularis mucosa was thicker, but the muscularis propria was thinner and the nuclei were smaller compared with the control group (Fig. 3F).

**Ultrastructure.** TEM was performed to observe the colon wall ultrastructure. In the control group (Fig. 4A), the smooth muscle cells were long, spindle-shaped and surrounded by collagen fibers (indicated by the black arrows; Fig. 4A). However, in the UC group (Fig. 4B), the cell shape was abnormal, and the cells appeared shorter and rounder. Additionally, the arrangement of the cells was irregular, and the collagen fibers (indicated by the black arrows; Fig. 4B) were rare. Collagen fibers surrounding the smooth muscle cells were tied into a compact bundle in the control group (indicated by the star; Fig. 4C), but in the UC group, the collagen fibers were looser, and the arrangement was irregular (indicated by the star; Fig. 4D). Changes in the smooth muscle cells were also observed. In the control group (Fig. 4E), the nuclear envelope of smooth muscle cells was complete (indicated by black arrows; Fig. 4E) and the nucleus was long and spindle-shaped with a small but

clear nucleolus (indicated by the triangle; Fig. 4E). Conversely, in the UC group (Fig. 4F), the smooth muscle cell was edematous, the nuclear envelope was unclear, and the shape of the nucleus was irregular and edematous.

## Discussion

DSS is regarded as the most effective way to generate a UC mouse model (13). The DSS-induced colitis model has certain advantages relative to other animal models of colitis. An acute, chronic or relapsing model can be easily produced by altering the concentration of DSS administered (20). Among these protocols, oral administration of DSS is regarded as a simple, economical and effective method in mice. The proposed and most accepted mechanism by which DSS induces intestinal inflammation is associated with the disruption of the intestinal epithelial monolayer lining, leading to the entry of luminal bacteria and associated antigens into the mucosa and allowing the dissemination of proinflammatory intestinal contents into underlying tissue (21). Histological investigation was performed on a mouse model in the present study to elucidate

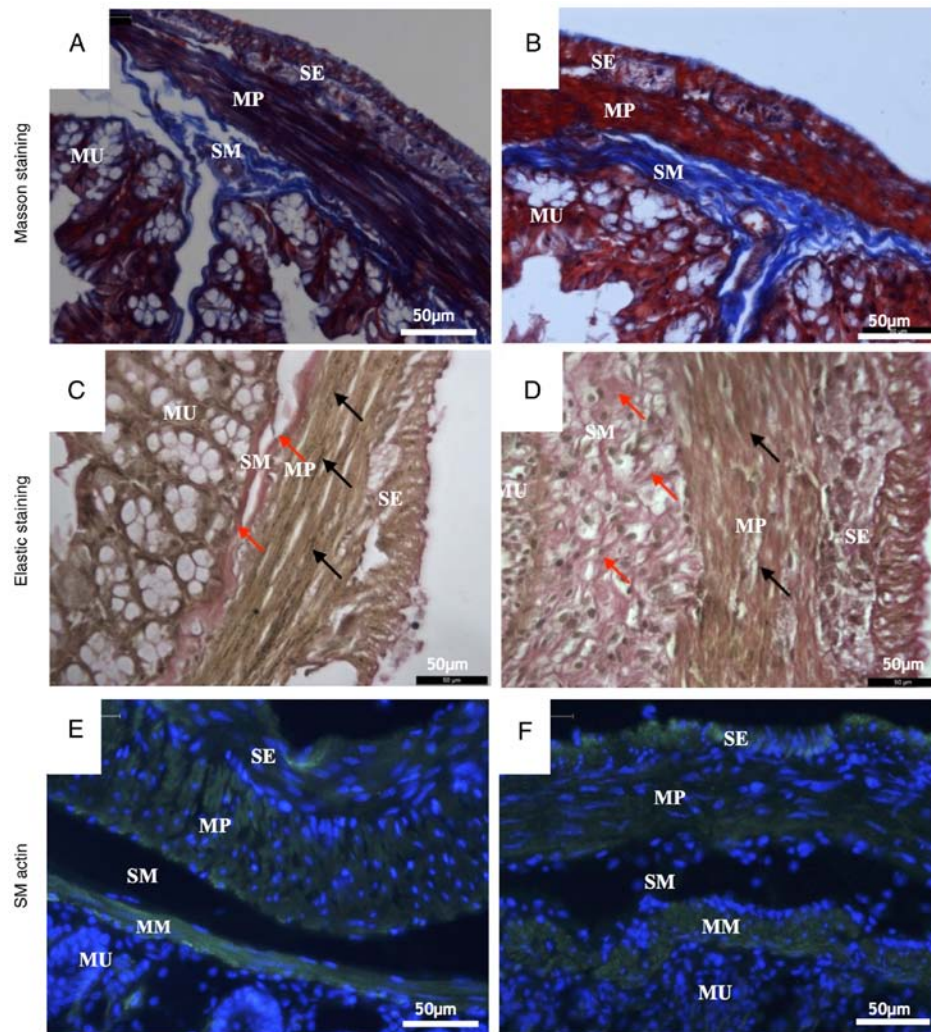


Figure 3. Representative histological images of colon walls. Masson staining images of (A) control and (B) UC mice. Elastic staining images of (C) control and (D) UC mice. Collagen fibers in submucosa are indicated by the red arrows. Elastic fibers in the muscularis propria are indicated by the black arrows. Smooth muscle actin staining images of (E) control and (F) UC mice. Magnification,  $\times 400$ . Scale bar,  $50 \mu\text{m}$ . UC, ulcerative colitis; MU, mucosa; SM, submucosa; MP, muscularis propria; SE, serosa.

changes in the microstructure of colon tissue in response to DSS-induced early-stage UC.

One way to diagnose and monitor inflammatory bowel disease (IBD) in the clinical setting, which mainly includes UC and CD, is by recording the clinical symptoms of the patient. Symptoms often related to UC include rectal bleeding or bloody diarrhea (22). The manifestations observed in DSS-induced mice used in the current study include weight loss, diarrhea, occult blood in stools and anemia, which were similar to those previously reported in the human UC case (23).

Histological features typical of IBD compared with other mucosal inflammations are epithelial distortions, such as crypt branching and shortening and decreased crypt density, and severe infiltration of inflammatory cells to the intestinal wall (20,24). Furthermore, a reduction in goblet cell numbers is typical for UC, but not for CD (25,26). Another typical histological feature found in patients with IBD is the severe infiltration of mononuclear cells and plasma cells into the basal lamina propria of the inflamed intestinal wall (25,26). The present study found irregular epithelial formation with crypt distortion and goblet cell depletion (data not shown), similar

to changes found in patients with UC (27,28). In addition, a high number of inflammatory cells infiltrated into the stroma and the structure of the gland was destroyed. The tissue in the submucosa showed significant edema due to inflammatory cell infiltration.

Fibrosis in UC is characterized by increased deposits of collagen in the submucosa and lamina propria (29). In the animal model used in the present study, an extensive deposition of collagen was detected in the mucosa and submucosa of acutely inflamed colons, resembling fibrosis in UC. In the current study, it was observed that the collagen fibers proliferated into the submucosa without a regulatory arrangement at the early stage of UC. They were loose, forming a disorganized fiber net instead of a fiber bundle. In the muscularis propria, the fibers, including both collagen and elastic fibers, were reduced and fractured. The above changes lead to insufficient intestinal motility.

In human UC, ultrastructure alterations of the epithelium have been observed, including microvilli depletion, shattering of the epithelial junctions, cytoplasmic vacuolization, dilatation of the endoplasmic reticulum, pyknotic nuclei and altered

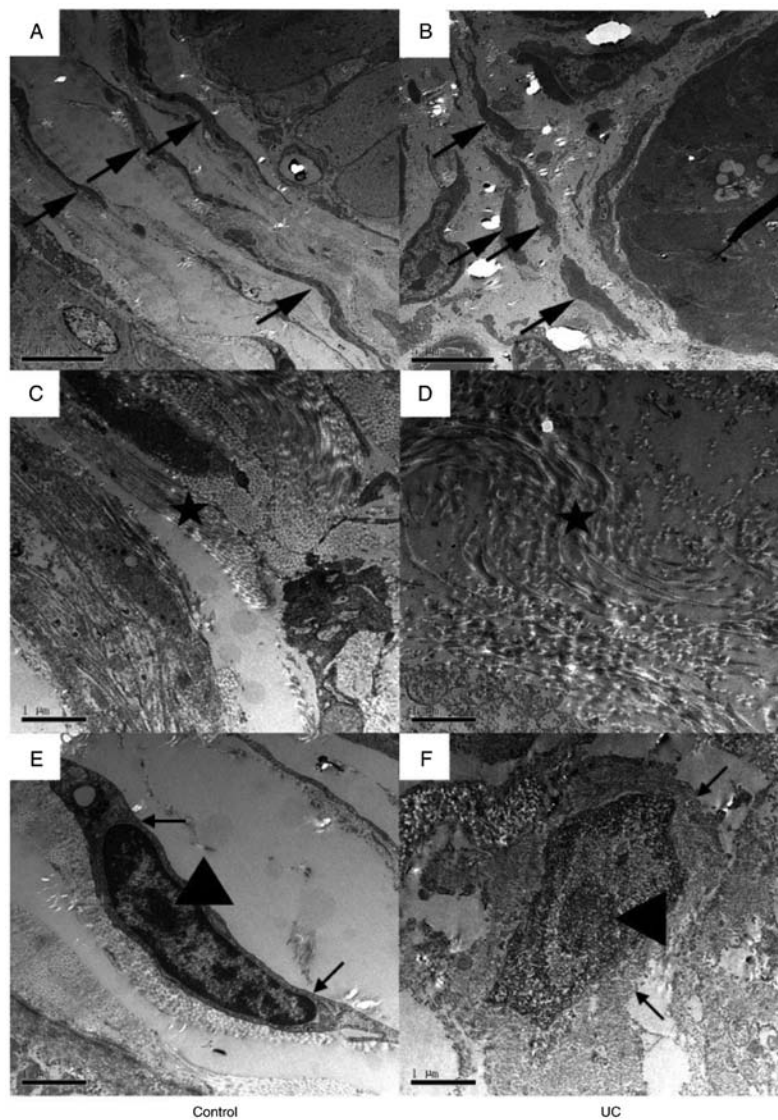


Figure 4. Representative transmission electron microscopy images of colon walls. Images of (A) control and (B) UC group colon samples at x5,000 magnification. Smooth muscle cells are indicated by the arrows. The smooth muscle cells were long spindle-shaped and surrounded by the collagen fibers in the control group, while they were shorter and rounder in the UC group. Scale bar, 5  $\mu\text{m}$ . Images of (C) control and (D) UC group samples at x20,000 magnification. Collagen fibers are indicated by the stars. The arrangement of each collagen fibers bundled along with the smooth muscle's axle in the control group, while the collagen fibers were much looser in the UC group. Scale bar, 1  $\mu\text{m}$ . Images of (E) control and (F) UC samples at x20,000 magnification. The nuclear envelope of smooth muscle cell was complete in the control group, and the nucleus was long and spindle-shaped with a small but clear nucleolus. However, in the UC group, the smooth muscle cell was edematous, the nuclear envelope was unclear, and the shape of the nucleus was irregular and edematous. Scale bar, 1  $\mu\text{m}$ . UC, ulcerative colitis.

structuring of the mitochondria and Golgi complexes (30,31). However, to the best of our knowledge, the ultrastructure of the muscularis propria has not been fully elucidated. The results of the present study found an irregular arrangement of the smooth muscle cells in the muscularis propria of the DSS-induced mouse model. These cells were rounder and shorter, and surrounded by looser and more irregular collagen fibers. Severe alterations of the cell membrane and nucleus were also observed. The changes observed among smooth muscle cells and collagen fibers indicated that the colon wall in UC was less resistant to external forces, as previously reported by the authors of the current study (32). Changes in the morphology of these cells may indicate epithelial cell injury.

Chemical reagents used for inducing colitis in animal models mainly include 2,4,6-trinitrobenzene sulfonic acid (TNBS), DSS and oxazolone (13,33,34). Both TNBS and

oxazolone-mediated colitis are induced by intrarectal administration of the reagents and the pathogenesis primarily involves a T cell-mediated response against autologous proteins or luminal antigens (10). However, in the DSS-induced colitis model, mice are treated with water supplemented with DSS for several days (10,20,24). DSS seems to play a directly toxic role in colonic epithelial cells of the basal crypts, and several immunological responses also play a role in the pathogenesis of UC (33). TNBS-induced colitis is thought to be a T helper (Th) cell-mediated disease, while Th2-relevant cytokine levels are increased in DSS- and oxazolone-induced colitis (33). Although the exact mechanisms differ, these three colitis-inducing chemical reagents in murine models share a number of similarities in terms of histology alterations (35,36). The infiltration of neutrophils and macrophages is observed as early as on the first day after chemical stimulation, and

the infiltration is increased over time (10). By day 3, ulcerations, goblet cell depletion and fibrosis are present in the colon (33,34). Farkas *et al* (37) observed leucocyte rolling, sticking and extravasation under an electron microscope. The present work further extended the understanding of ultrastructure alterations in DSS-induced colitis. The ultrastructure alterations found in the current DSS-induced model might also be found in other reagent-induced colitis models, since the three chemical-induced colitis murine models share similar pathological injuries under light microscopy (35). It is worth further investigating the ultrastructure of other reagent-induced colitis models in order for the characteristics of the three models to be compared. Additionally, colitis research can be improved through choosing more suitable colitis models, such as congenital and adaptive cell transferred models (38).

In conclusion, UC was successfully induced with 7 consecutive days of DSS oral administration in mice. The ultrastructure changes of DSS-induced UC colon were examined. Experimental DSS-induced colitis in mice shared most features with human UC. These features may contribute to improved understanding of the pathogenesis and mechanism of UC.

### Acknowledgements

Not applicable.

### Funding

This work was supported by grants from the National Natural Science Foundation of China (grant nos. 31571181 and 11702197) and the Fundamental Research Funds for the Central Universities (grant nos. 22120180077 and 1500219128).

### Availability of data and materials

The datasets used and/or analyzed during the current study are available from the corresponding author on reasonable request.

### Authors' contributions

XX and YL conceived and designed the study. XX, SL, JT, YY, XG and KL performed the experiments and analyzed the data. XX, SL, JT and YL wrote and revised the manuscript. All authors read and approved the final manuscript.

### Ethics approval and consent to participate

All experimental procedures were performed according to International Guidelines for the Care and Use of Laboratory Animals and were approved by the Animal Ethics Committee of Tongji University School of Medicine, Shanghai, China (approval no. TJLAC-014-015).

### Patient consent for publication

Not applicable.

### Competing interests

The authors declare that they have no competing interests.

### References

1. Ungaro R, Mehandru S, Allen PB, Peyrin-Biroulet L and Colombel JF: Ulcerative colitis. *Lancet* 389: 1756-1770, 2017.
2. da Silva BC, Lyra AC, Rocha R and Santana GO: Epidemiology, demographic characteristics and prognostic predictors of ulcerative colitis. *World J Gastroenterol* 20: 9458-9467, 2014.
3. Adams SM and Bornemann PH: Ulcerative colitis. *Am Fam Physician* 87: 699-705, 2013.
4. Di Sabatino A, Biancheri P, Rovedatti L, Macdonald TT and Corazza GR: Recent advances in understanding ulcerative colitis. *Intern Emerg Med* 7: 103-111, 2012.
5. Maul J and Zeitz M: Ulcerative colitis: Immune function, tissue fibrosis and current therapeutic considerations. *Langenbecks Arch Surg* 397: 1-10, 2012.
6. Rieder F and Fiocchi C: Intestinal fibrosis in inflammatory bowel disease - Current knowledge and future perspectives. *J Crohn's Colitis* 2: 279-290, 2008.
7. Manetti M, Rosa I, Messerini L and Ibba-Manneschi L: Telocytes are reduced during fibrotic remodelling of the colonic wall in ulcerative colitis. *J Cell Mol Med* 19: 62-73, 2015.
8. Chassaing B and Darfeuille-Michaud A: The commensal microbiota and enteropathogens in the pathogenesis of inflammatory bowel diseases. *Gastroenterology* 140: 1720-1728, 2011.
9. Rijnierse A, Nijkamp FP and Kraneveld AD: Mast cells and nerves tickle in the tummy: Implications for inflammatory bowel disease and irritable bowel syndrome. *Pharmacol Ther* 116: 207-235, 2007.
10. Randhawa PK, Singh K, Singh N and Jaggi AS: A review on chemical-induced inflammatory bowel disease models in rodents. *Korean J Physiol Pharmacol* 18: 279-288, 2014.
11. Whittam CG, Williams AD and Williams CS: Murine Colitis modeling using Dextran Sulfate Sodium (DSS). *J Vis Exp* 35: 1652, 2010.
12. Okayasu I, Hatakeyama S, Yamada M, Ohkusa T, Inagaki Y and Nakaya R: A novel method in the induction of reliable experimental acute and chronic ulcerative colitis in mice. *Gastroenterology* 98: 694-702, 1990.
13. Chassaing B, Aitken JD, Malleshappa M and Vijay-Kumar M: Dextran sulfate sodium (DSS)-induced colitis in mice. *Curr Protoc Immunol* 104. Unit 15: 25, 2014.
14. Alleva E and Santucci D: Guide for the care and use of laboratory animals. *Ethology* 103: 1072-1073, 1997.
15. Li YY, Yuece B, Cao HM, Lin HX, Lv S, Chen JC, Ochs S, Sibae A, Deindl E, Schaefer C, *et al*: Inhibition of p38/Mk2 signaling pathway improves the anti-inflammatory effect of WIN55 on mouse experimental colitis. *Lab Invest* 93: 322-333, 2013.
16. Kimball ES, Wallace NH, Schneider CR, D'Andrea MR and Hornby PJ: Vanilloid receptor 1 antagonists attenuate disease severity in dextran sulphate sodium-induced colitis in mice. *Neurogastroenterol Motil* 16: 811-818, 2004.
17. Engel MA, Kellermann CA, Rau T, Burnat G, Hahn EG and Konturek PC: Ulcerative colitis in AKR mice is attenuated by intraperitoneally administered anandamide. *J Physiol Pharmacol* 59: 673-689, 2008.
18. Ippolito C, Colucci R, Segnani C, Errede M, Girolamo F, Virgintino D, Dolfi A, Tirota E, Buccianti P, Di Candio G, *et al*: Fibrotic and Vascular Remodelling of Colonic Wall in Patients with Active Ulcerative Colitis. *J Crohn's Colitis* 10: 1194-1204, 2016.
19. Lai S, Yu W, Wallace L and Sigalet D: Intestinal muscularis propria increases in thickness with corrected gestational age and is focally attenuated in patients with isolated intestinal perforations. *J Pediatr Surg* 49: 114-119, 2014.
20. Melgar S, Karlsson A and Michaëlsson E: Acute colitis induced by dextran sulfate sodium progresses to chronicity in C57BL/6 but not in BALB/c mice: Correlation between symptoms and inflammation. *Am J Physiol Gastrointest Liver Physiol* 288: G1328-G1338, 2005.
21. Rath HC, Schultz M, Freitag R, Dieleman LA, Li F, Linde HJ, Schölmerich J and Sartor RB: Different subsets of enteric bacteria induce and perpetuate experimental colitis in rats and mice. *Infect Immun* 69: 2277-2285, 2001.
22. Baumgart DC and Sandborn WJ: Inflammatory bowel disease: Clinical aspects and established and evolving therapies. *Lancet* 369: 1641-1657, 2007.
23. Perše M and Cerar A: Dextran sodium sulphate colitis mouse model: Traps and tricks. *J Biomed Biotechnol* 2012: 718617, 2012.

24. Taghipour N, Molaei M, Mosaffa N, Rostami-Nejad M, Asadzadeh Aghdaei H, Anissian A, Azimzadeh P and Zali MR: An experimental model of colitis induced by dextran sulfate sodium from acute progresses to chronicity in C57BL/6: Correlation between conditions of mice and the environment. *Gastroenterol Hepatol Bed Bench* 9: 45-52, 2016.
25. Tanaka M, Riddell RH, Saito H, Soma Y, Hidaka H and Kudo H: Morphologic criteria applicable to biopsy specimens for effective distinction of inflammatory bowel disease from other forms of colitis and of Crohn's disease from ulcerative colitis. *Scand J Gastroenterol* 34: 55-67, 1999.
26. Geboes K and Dalle I: Influence of treatment on morphological features of mucosal inflammation. *Gut* 50 (Suppl 3): III37-III42, 2002.
27. Allison MC, Hamilton-Dutoit SJ, Dhillon AP and Pounder RE: The value of rectal biopsy in distinguishing self-limited colitis from early inflammatory bowel disease. *Q J Med* 65: 985-995, 1987.
28. Theodossi A, Spiegelhalter DJ, Jass J, Firth J, Dixon M, Leader M, Levison DA, Lindley R, Filipe I and Price A: Observer variation and discriminatory value of biopsy features in inflammatory bowel disease. *Gut* 35: 961-968, 1994.
29. Matthes H, Herbst H, Schuppan D, Stallmach A, Milani S, Stein H and Riecken EO: Cellular localization of procollagen gene transcripts in inflammatory bowel diseases. *Gastroenterology* 102: 431-442, 1992.
30. Rumessen JJ: Ultrastructure of interstitial cells of Cajal at the colonic submuscular border in patients with ulcerative colitis. *Gastroenterology* 111: 1447-1455, 1996.
31. Fratila OC and Craciun C: Ultrastructural evidence of mucosal healing after infliximab in patients with ulcerative colitis. *J Gastrointest Liver Dis* 19: 147-153, 2010.
32. Gong X, Xu X, Lin S, Cheng Y, Tong J and Li Y: Alterations in biomechanical properties and microstructure of colon wall in early-stage experimental colitis. *Exp Ther Med* 14: 995-1000, 2017.
33. Alex P, Zachos NC, Nguyen T, Gonzales L, Chen TE, Conklin LS, Centola M and Li X: Distinct cytokine patterns identified from multiplex profiles of murine DSS and TNBS-induced colitis. *Inflamm Bowel Dis* 15: 341-352, 2009.
34. Wirtz S, Popp V, Kindermann M, Gerlach K, Weigmann B, Fichtner-Feigl S and Neurath MF: Chemically induced mouse models of acute and chronic intestinal inflammation. *Nat Protoc* 12: 1295-1309, 2017.
35. Goyal N, Rana A, Ahlawat A, Bijjem KR and Kumar P: Animal models of inflammatory bowel disease: A review. *Inflammopharmacology* 22: 219-233, 2014.
36. Sartor RB: Review article: How relevant to human inflammatory bowel disease are current animal models of intestinal inflammation? *Aliment Pharmacol Ther* 11 (Suppl 3): 89-96, discussion 96-97, 1997.
37. Farkas S, Herfarth H, Rössle M, Schroeder J, Steinbauer M, Guba M, Beham A, Schölmerich J, Jauch KW and Anthuber M: Quantification of mucosal leucocyte endothelial cell interaction by *in vivo* fluorescence microscopy in experimental colitis in mice. *Clin Exp Immunol* 126: 250-258, 2001.
38. Mizoguchi E, Low D, Ezaki Y and Okada T: Recent updates on the basic mechanisms and pathogenesis of inflammatory bowel diseases in experimental animal models. *Intest Res* 18: 151-167, 2020.



This work is licensed under a Creative Commons Attribution-NonCommercial-NoDerivatives 4.0 International (CC BY-NC-ND 4.0) License.